BBA - Molecular Basis of Disease 1864 (2018) 2409–2419

Contents lists available at ScienceDirect

BBA - Molecular Basis of Disease

journal homepage: www.elsevier.com/locate/bbadis

TRPM7 controls mesenchymal features of breast cancer cells by tensional regulation of SOX4

Arthur J. Kuipers[a,1], Jeroen Middelbeek[a,1], Kirsten Vrenken[a], Carlos Pérez-González[b,c], Geert Poelmans[d,e], Jeffrey Klarenbeek[f], Kees Jalink[f], Xavier Trepat[b,c,g,h], Frank N. van Leeuwen[a,*]

[a] Laboratory of Pediatric Oncology, Radboud Institute for Molecular Life Sciences, Radboud university medical center, Nijmegen, The Netherlands
[b] Institute for Bioengineering of Catalonia (IBEC), 08028 Barcelona, Spain
[c] University of Barcelona, Barcelona 08028, Spain
[d] Department of Human Genetics, Radboud university medical center, Nijmegen, The Netherlands
[e] Department of Molecular Animal Physiology, Donders Institute for Brain, Cognition and Behaviour, Radboud University, Nijmegen, The Netherlands
[f] Division of Cell Biology, Netherlands Cancer Institute, Amsterdam, The Netherlands
[g] Institució Catalana de Recerca i Estudis Avançats (ICREA), Barcelona 08010, Spain
[h] Centro de Investigación Biomédica en Red en Bioingeniería (CIBER), Biomateriales y Nanomedicina, Barcelona 08028, Spain

ARTICLE INFO

Keywords:
TRPM7
SOX4
Epithelial-mesenchymal transition
Cytoskeleton
Mechanotransduction

ABSTRACT

Mechanically induced signaling pathways are important drivers of tumor progression. However, if and how mechanical signals affect metastasis or therapy response remains poorly understood. We previously found that the channel-kinase TRPM7, a regulator of cellular tension implicated in mechano-sensory processes, is required for breast cancer metastasis *in vitro* and *in vivo*. Here, we show that TRPM7 contributes to maintaining a mesenchymal phenotype in breast cancer cells by tensional regulation of the EMT transcription factor SOX4. The functional consequences of SOX4 knockdown closely mirror those produced by TRPM7 knockdown. By traction force measurements, we demonstrate that TRPM7 reduces cytoskeletal tension through inhibition of myosin II activity. Moreover, we show that SOX4 expression and downstream mesenchymal markers are inversely regulated by cytoskeletal tension and matrix rigidity. Overall, our results identify SOX4 as a transcription factor that is uniquely sensitive to cellular tension and indicate that TRPM7 may contribute to breast cancer progression by tensional regulation of SOX4.

1. Introduction

The perception of mechanical cues from the microenvironment by cell adhesion sites is essential for morphogenesis during embryonic development, and for maintenance of tissue integrity and function in the adult [1–9]. Typically, mechanical stress triggers an immediate internal feedback loop that evokes cytoskeletal contraction and enforcement of adhesions sites to restore tensional homeostasis [10–13]. As a more sustained effect, mechano-signaling regulates gene expression programs that steer proliferation and differentiation [14–16]. Consequently, perturbed mechano-signaling contributes to a variety of pathologies, including tissue fibrosis and cancer [17,18].

In order to metastasize or escape therapy, tumor cells can re-acquire progenitor-like features. Soluble factors present in the tumor microenvironment such as TGF-β and Wnt proteins, as well as mechanical crosstalk between tumor cells and the surrounding tissue, can bring about this progenitor-like state [19]. For instance, mechanically-regulated signaling pathways such as those mediated by YAP/TAZ or myocardin-related transcription factor/serum response factor (MRTF/SRF) are essential in the control of stem cell development but, when spuriously activated by increased cellular tension, contribute to tumor progression [17,20,21]. More recently, changes in cellular tension were shown to affect epithelial-mesenchymal transition (EMT), a developmental transcription program co-opted by tumor cells to acquire migratory properties, survive outside of their niche, and resist therapy [22–25]. However, many aspects of these mechanically-regulated signaling pathways remain poorly understood.

Transient receptor potential (TRP) cation channels are considered important transducers of mechanical signals during embryonic development and in the maintenance of tissue homeostasis [26]. Localized

* Corresponding author at: Laboratory of Pediatric Oncology, Radboud Institute For Molecular Life Sciences, Radboud university medical center, PO Box 9101, 6500 HB Nijmegen, The Netherlands.
E-mail address: FrankN.vanLeeuwen@radboudumc.nl (F.N. van Leeuwen).
[1] Contributed equally

https://doi.org/10.1016/j.bbadis.2018.04.017
Received 17 November 2017; Received in revised form 13 April 2018; Accepted 18 April 2018
Available online 21 April 2018

within mechano-sensory structures such as cell adhesions, channel opening is induced by membrane stretch and/or cytoskeletal tension [27]. The resulting changes in local ion concentrations not only trigger immediate cytoskeletal responses, but also bring about more sustained effects by regulating gene expression [26–29].

TRPM7, a calcium-permeable TRP channel with a functional C-terminal kinase domain that localizes to cell adhesion sites, is required during embryogenesis and maintains stem cell-like features of progenitor cells [30–34]. We previously demonstrated that expression of TRPM7 is required for breast tumor cell migration *in vitro* and metastasis formation in mouse xenografts [35]. In addition, high *TRPM7* mRNA expression at time of diagnosis predicts metastasis formation and poor outcome in breast cancer patients [35]. The association between high *TRPM7* expression and cancer progression has been confirmed in other tumor types, including neuroblastoma, pancreatic, nasopharyngeal and prostate cancer [36–39]. In previous studies, we and others demonstrated that TRPM7 activity affects cell adhesion and migration by reducing myosin II-based cellular tension [27,40–42]. As TRPM7 was shown to affect cellular differentiation [31,32,39], we postulate that TRPM7-induced changes in cytoskeletal tension have long-term effects on the progenitor features of tumor cells by (re)activating developmental gene expression programs.

Here, we report that TRPM7 contributes to the mesenchymal features of breast cancer cell lines by regulating expression of the transcription factor SOX4, an important driver of EMT in breast cancer cells that is implicated in breast cancer progression [43,44]. We further demonstrate that expression of SOX4 is inversely regulated by actomyosin-based contraction and matrix rigidity. Consequently, our observations suggest a model in which limiting the contractile response to tissue stiffness activates a SOX4-mediated gene expression program. As SOX4 activation has been linked to metastatic progression [43,44], TRPM7-mediated mechanical regulation of this transcription factor may contribute to the cellular plasticity observed during breast cancer progression.

2. Materials and methods

2.1. Antibodies and reagents

Reagents: Waixenicin A was a kind gift from David Horgen (Hawaii Pacific University, Kaneohe, U.S.A.). From Sigma-Aldrich: LPA (#L7260), Y-27632 (#Y0503), blebbistatin (#B0560), 4-OHT (#H6278).

Antibodies: From Cell Signaling Technology: Claudin-1 (#4933, WB 1:1000), E-cadherin (#3195, WB 1:2000), ZO-1 (#8193, WB 1:2000; IF 1:200). From BD Biosciences: fibronectin (#610077, WB 1:5000, IF 1:500), vimentin (#550513, WB 1:5000). From Sigma-Aldrich: γ-tubulin (#T6557, WB 1:10000), vinculin (#V9131, IF 1:400). From Diagenode: SOX4 (#C15310129, WB 1:4000). From Life Technologies – Molecular Probes: phalloidin-Alexa-568 (#A12380, IF 1:200).

2.2. Cell culture

MDA-MB-231 and Hs 578T (American Type Culture Collection) were cultured in Dulbecco's Modified Eagle Medium + Glutamax (Life Technologies, Gibco, #31966), supplemented with 10% heat-inactivated fetal bovine serum and 1% pen/strep (Life Technologies, Invitrogen, #15140). Cells were cultured in a humidified incubator at 37 °C and 5% CO_2.

2.3. Generation of cell lines

To generate knockdown cell lines control, TRPM7 [35] or SOX4 shRNAs (obtained from Dr. R. Beijersbergen at The Netherlands Cancer Institute - Screening and Robotics Facility) (see Supplementary Table 2 for sequences) were transduced into MDA-MB-231 or Hs 578T cells using the pLKO lentiviral expression vector according to manufacturer's protocol (Sigma-Aldrich). Cells were selected using 1 μg/ml puromycin. To generate a stable constitutively active RhoA overexpressing cell line, MDA-231 shControl cells were transduced with pLZRS-mycV14RhoA or an empty vector control. Cells were selected with 2 mg/ml G418. Stable overexpression of SOX4 in shControl and shTRPM7 cells was obtained by expression of the pBABE-blast ER and pBABE-blast ER:SOX4 constructs generated in the lab of Prof. P. J. Coffer (UMC Utrecht, Utrecht, The Netherlands) [51]. These constructs encode the hormone-binding domain of the human estrogen receptor (ER) or a fusion protein of mouse Sox4 with the hormone-binding domain of the human estrogen receptor, respectively. Cells were selected with 20 μg/ml blasticidin. For each experiment, cells were stimulated with 100 nM 4-hydroxy tamoxifen (4-OHT) for 24 h.

2.4. Immunofluorescence

For staining of cell-cell contacts and fibronectin, cells were cultured o/n on glass coverslips. For quantification of cell-matrix adhesion size, cells were cultured on collagen-coated polyacrylamide gels. Cells were subsequently fixed in 4% paraformaldehyde and permeabilized in 0.1% Triton-X 100. Non-specific binding was blocked with 3% BSA. Cells were incubated with ZO-1, fibronectin-1 or vinculin antibodies diluted in 3% BSA. Cells were then incubated with phalloidin-Alexa 568 and anti-rabbit Alexa 647 conjugated antibodies diluted in 3% BSA. Images (2048 × 2048 resolution, with 6× line averaging) were taken on a Leica TCS SP5 (Leica Microsystems) equipped with a 63× water-immersion objective and LAS-AF acquisition software (Leica Microsystems). Images were processed for publication using ImageJ 1.48.

2.5. Quantitative real-time PCR

mRNA was isolated using an RNeasy minikit (Qiagen, #74106) and DNAse-treated on column (Qiagen, #79254). cDNA was synthesized using an iScript cDNA synthesis kit according to manufacturer's protocol (Bio-Rad, #170-8891). q-PCRs were performed using Power SYBR green mix (Life Technologies, Applied Biosystems, #4368708) on a CFX96 Touch™ Real-Time System (Bio-Rad) using PCR conditions as supplied by Applied Biosystems. Gene expression levels were normalized against the GAPDH housekeeping gene and calculated according to the $2^{-\Delta\Delta Ct}$ method. For q-PCR primer sequences, see Supplementary Table 2.

2.6. Western blotting

Cells were lysed in RIPA lysis buffer (150 mM NaCl, 1% NP40, 5 mM EDTA, 50 mM Tris pH 8.0, 0.5% deoxycholate, 0.1% SDS) supplemented with complete protease inhibitor cocktail (Roche). After clarification, lysates were diluted in Laemmli's buffer (0.25 M Tris pH 6.8, 10% glycerol, 2% SDS and 0.02% bromophenol blue), supplemented with 10% β-mercaptoethanol and incubated at 95 °C for 5 min. Proteins were separated by SDS-PAGE and subsequently blotted onto PVDF membranes. Non-specific binding was blocked with 5% BSA or 4% skim milk (for SOX4 blots) diluted in TBS + 0.1% Tween-20 (TBST). Blots were then incubated with primary antibodies, followed by HRP-conjugated secondary antibodies, diluted in TBST + 5% BSA or 0.8% skim milk (for SOX4 blots). Proteins were detected using ECL detection agent (Amersham GE Healthcare #RPN2232) and imaged on a Fluorchem E Digital Darkroom (Proteinsimple).

2.7. Microarray analysis

MDA-231 shCntrl, shTRPM7 and shSOX4#1 were subjected to microarray analysis (GEO accession number: GSE63958), which was performed at Genomescan B.V. (Leiden, The Netherlands). RNA

concentrations were measured using the Nanodrop ND-1000 spectrophotometer (Nanodrop Technologies). RNA quality and integrity were determined using Lab-on-Chip analysis on the Agilent 2100 Bioanalyzer (Agilent Technologies). Biotinylated cRNA was prepared using the Illumina TotalPrep RNA Amplification Kit (Ambion Inc.) according to manufacturer's specifications with an input of 200 ng total RNA. Per sample, 750 ng of the obtained biotinylated cRNA samples was hybridized onto the Illumina HumanHT-12 v4 (Illumina Inc.). Hybridization and washing were performed according to the Illumina Manual 'Direct Hybridization Assay Guide'. Scanning was performed on the Illumina iScan (Illumina Inc.). Image analysis and extraction of raw expression data was performed with Illumina GenomeStudio v2011.1 Gene Expression software. Arrays were normalized in Arraystar (v. 4.03), using Robust-Multi-Array normalization. For visualization of selected EMT/MET inducers in a heatmap (Multi Experiment Viewer v 4.8.1), normalized linear intensity values were $\log_{10}$ transformed. Statistical significance of overlapping up- and downregulated in MDA-231 shTRPM7 and shSOX4#1 was determined by means of a hypergeometric distribution test. To this end, normalized linear intensity values were $\log_2$ transformed. $\log_2$ values < 2.5 were considered background and a fold change of $\geq |2|$ was used as cut-off. The amount of background corrected gene products (n = 22,278) was used as total gene set for the hypergeometric distribution test.

2.8. Preparation of polyacrylamide gels

Polyacrylamide gels were prepared as previously described [10]. Briefly, glass-bottom dishes (MatTek) were activated with a solution of 3-(trimethoxysilyl)propyl methacrylate (Sigma-Aldrich), acetic acid and ethanol (1:1:14), washed with ethanol and air-dried for 10 min. To generate gels of different stiffness, different concentrations of acrylamide and bis-acrylamide were mixed in 10 mM HEPES supplemented with 0.5% ammonium persulfate, 0.05% tetramethylethylenediamine (Sigma) and 0.4% fluorescent red carboxylated nanobeads (Invitrogen) (see Supplementary Table 3). 10 μl of this solution was then placed on the center of the glass-bottom dishes and covered with 12-mm-diameter glass coverslips. After gel polymerization, top coverslips were removed and gels were incubated with 100 μg/ml Collagen (Nalgene) overnight at 4 °C. After washing gels with PBS, cells were then trypsinized and plated on gels. For traction force measurements and immunostaining, cells were cultured for 2–4 h. For mRNA expression analysis, cells were cultured for 72 h.

2.9. Traction force microscopy

Traction force measurements were performed as described previously [10]. Cells seeded on gels were placed on an inverted microscope (Nikon Eclipse Ti). Phase contrast images of single cells and fluorescence images of the embedded nanobeads were obtained with a 40× objective (NA 0.6). At the end of the measurements, cells were trypsinized and an image of bead positions in the relaxed state of the gel was acquired. By comparing bead positions with and without cells, a map of gel deformations caused by cells was first obtained using custom particle imaging velocimetry software [78]. Then, after assuming that gel displacements were caused by forces exerted by cells in the cell–gel contact area, the corresponding map of cell forces was calculated using a previously described Fourier transform algorithm [56,79]. The average forces per unit area exerted by each cell were then calculated. To calculate the minimum detectable force levels for each rigidity, we followed the same procedure in cell-free gel areas, and calculated the resulting forces. Phase contrast images were also used to calculate average cell spreading areas as a function of substrate stiffness.

2.10. Statistical analysis

Statistics on q-PCR data were performed using a one-sample *t*-test, comparing fold changes in expression to control levels that were set to 1 in each independent experiment. Statistics on the effect of substrate stiffness on traction force generation, focal adhesion assembly and gene expression were performed using a two-way ANOVA. Data are represented as mean ± SEM. p-Values < 0.05 were considered statistically significant.

3. Results

3.1. TRPM7 maintains the mesenchymal phenotype of breast cancer cells

We previously showed that loss of TRPM7 expression impairs the metastatic potential of highly invasive MDA-MB-231 (MDA-231) breast cancer cells [35]. Knockdown of TRPM7 in MDA-231 cells using two independent shRNAs targeting TRPM7 resulted in a loss of the typical spindle-shaped morphology of these mesenchymal-type cells (Fig. 1A & [35]). TRPM7 has been linked to the regulation of cellular differentiation and embryonic development [31,32,34,45]. Moreover, TRPM7 was shown to regulate EMT in bladder cancer cells [46] and expression of the EMT marker vimentin in MDA-MB-468 breast cancer cells [47]. We therefore speculated that the effect of TRPM7 knockdown on the morphology of MDA-231 cells could represent a (partial) mesenchymal to epithelial transition (MET). Indeed, MDA-231 shTRPM7 cells showed increased formation of cell-cell adhesions, as observed by translocation of the tight junction protein ZO-1 to sites of cell-cell contacts (Fig. 1B), while the expression of ZO-1 was not affected (Fig. 1D). In addition, TRPM7 knockdown markedly increased the expression of the epithelial markers and cell-cell adhesion proteins E-cadherin (*CDH1*) and claudin-1 (*CLDN1*), both at the mRNA and protein level (Fig. 1C–D), whereas expression of the mesenchymal markers fibronectin (*FN1*) and vimentin (*VIM*) decreased (Fig. 1C–D & Supplementary Fig. 1A). N-cadherin (*CDH2*), which is known to respond in an inverse manner to E-cadherin expression, did not significantly decrease upon TRPM7 knockdown (data not shown). These observations were largely reproduced by incubating cells with the TRPM7-specific inhibitor Waixenicin A (Waix A) [48], which led to an increase in *CLDN1* expression and a decrease in *FN1* expression (Supplementary Fig. 1B). Unexpectedly however, *CDH1* expression decreased in response to Waix A treatment (Supplementary Fig. 1B). *TRPM7* mRNA remained unaffected by Waix A treatment expression (Supplementary Fig. 1B), consistent with the notion that Waix A affects TRPM7 activity rather than gene expression. Importantly, TRPM7 knockdown as well as inhibition of TRPM7 with Waix A induced a similar epithelial-like transition in the mesenchymal-type breast cancer cell line Hs 578T (Supplementary Fig. 2A–E). Taken together, these results indicate that TRPM7 is required for the maintenance of a mesenchymal phenotype of breast cancer cells, although loss of TRPM7 expression or activity is not sufficient to acquire a complete epithelial-like state.

3.2. TRPM7 regulates expression of the EMT transcription factor SOX4

To further investigate how TRPM7 maintains mesenchymal properties of breast cancer cells, we performed microarray analysis comparing MDA-231 shControl and shTRPM7 cells focusing on a set of transcription factors implicated in EMT or MET (EMT-TF) [49,50]. While inducers of MET remained largely unaffected, we found that the transcription factor SOX4 was most significantly downregulated in response to TRPM7 knockdown (~6×) (Fig. 2A). SOX4 was previously identified as an important determinant of EMT, affecting tumor cell migration and metastasis in mouse experimental metastasis models [43]. Moreover, and similar to TRPM7 [35], high SOX4 expression was found to correlate with metastatic progression in breast cancer patients [43]. Reduced expression of *SOX4* in response to TRPM7 shRNA-mediated knockdown was confirmed at both mRNA and protein level in MDA-231 and Hs 578T cells (Fig. 2B–C & Supplementary Fig. 3A–B). To

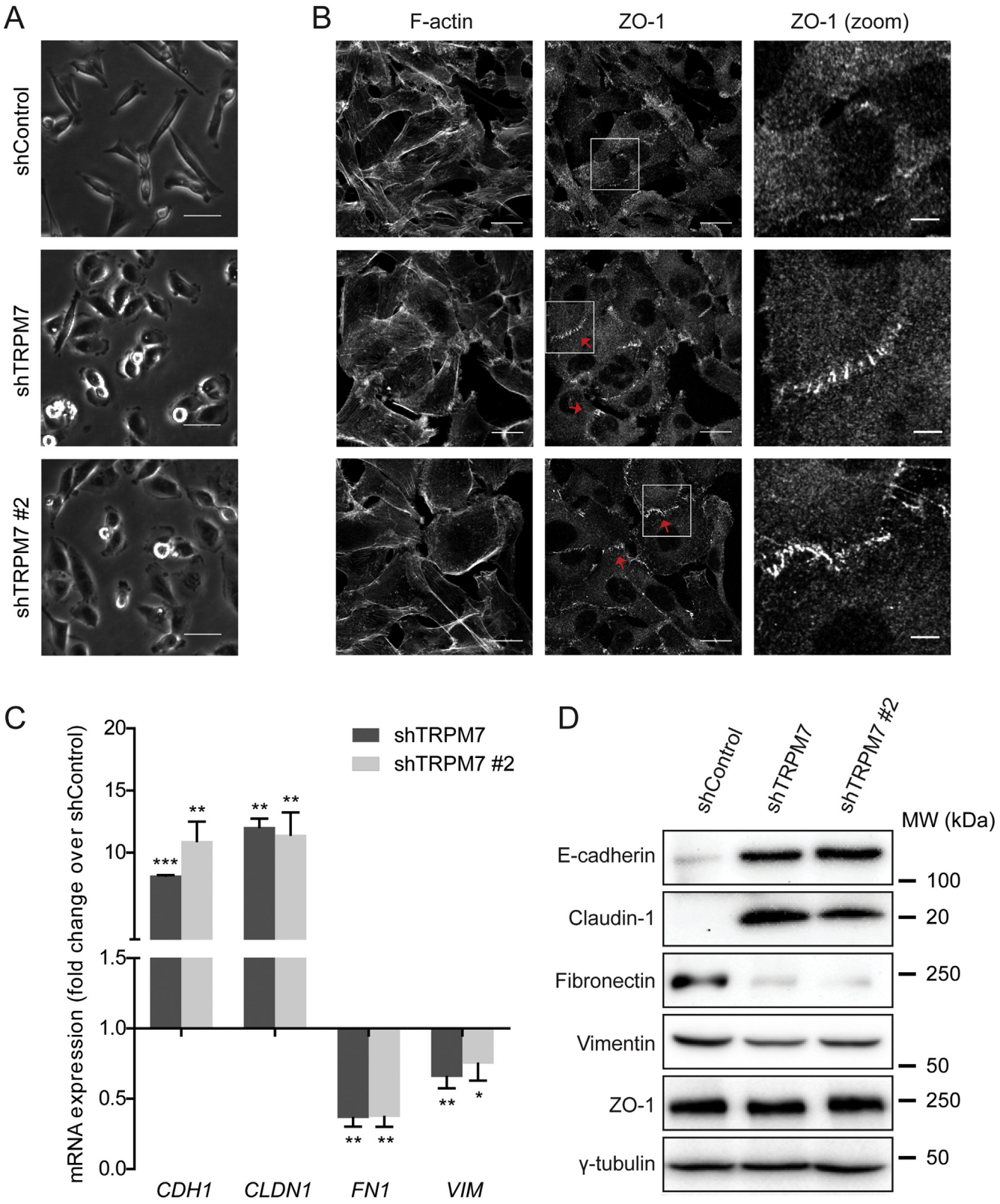

Fig. 1. TRPM7 is necessary for maintenance of the mesenchymal phenotype of MDA-231 cells. (A) Phase-contrast images showing morphology of MDA-231 shControl, shTRPM7 and shTRPM7#2. Scale bar = 50 μM. (B) Representative immunofluorescence staining of F-actin (cytoskeletal protein) and ZO-1 (tight junction protein). Red arrows in ZO-1 pictures indicate ZO-1 localization to cell-cell adhesions. Right panels are a zoom in of middle panels. Scale bars = 20 μM for left and middle panels, 5 μM for right panels. (C) Relative mRNA expression of indicated EMT markers, depicted as fold changes in expression over MDA-231 shControl as determined by q-PCR. Data are mean ± SEM of n = 3 experiments that were performed in duplicate. Statistical significance was determined by a one-sample *t*-test. * = $p < 0.05$, ** = $p < 0.01$, *** = $p < 0.001$. (D) Protein expression of indicated EMT markers as determined by Western blotting. γ-Tubulin was used as loading control. Representative examples of n = 3 experiments.

further substantiate the results from our gene expression profiling, we determined the expression of the well-established EMT-TFs *SNAI1*, *SNAI2*, *ZEB1* and *ZEB2* by q-PCR (*TWIST1* expression was not detected in MDA-231 cells) and observed that *SNAI2* expression was only weakly (< 2-fold) downregulated by TRPM7 knockdown in MDA-231 cells (Fig. 2B), but not in Hs 578T cells (Supplementary Fig. 3A). Similarly, inhibition of TRPM7 by treating MDA-231 and Hs 578T cells with Waix A induced a decrease in *SOX4* expression within hours after incubation with Waix A, while the expression of *SNAI2* remained largely unaffected (Fig. 2D & Supplementary Fig. 3C). Together, these results indicate that SOX4 is a common downstream transcriptional target of TRPM7 signaling in mesenchymal-type breast cancer cell lines. In further support of these observations, we found that *TRPM7* and *SOX4* mRNA expression are positively correlated in primary breast tumor samples, as determined in four independent, publicly available breast cancer patient cohorts (R2: Genomics Analysis and Visualization Platform, http://r2.amc.nl) (Fig. 2E).

3.3. SOX4 maintains the mesenchymal phenotype of breast cancer cells

To test whether reduced SOX4 expression induces a similar MET-like process in MDA-231 cells, we performed shRNA-mediated knockdown of SOX4 using two independent SOX4 targeting shRNAs (Supplementary Fig. 4A–B). Similar to TRPM7 knockdown cells, MDA-231 shSOX4 cells adopted an epithelial cell-like morphology (Fig. 3A) accompanied by a translocation of ZO-1 to sites of cell-cell contacts (Supplementary Fig. 4C). In addition, the expression of the cell-cell adhesion proteins E-cadherin and claudin-1 was strongly induced in MDA-231 shSOX4 cells, both at the mRNA and protein level (Fig. 3B–C). However, although N-cadherin was previously reported to be induced upon SOX4-mediated EMT [43], we did not observe a significant effect on N-cadherin expression levels upon SOX4 knockdown (data not shown). The second hairpin (shSOX4#2) produced a similar but less pronounced increase in E-cadherin and claudin-1, which most likely reflects a less efficient knockdown of SOX4 in these cells (Fig. 3B–C & Supplementary Fig. 4A–B). Fibronectin expression decreased to a similar extent in both SOX4 shRNA MDA-231 cell lines (Fig. 3B–C). No decrease in vimentin expression was observed (Fig. 3B–C). Expression of other EMT-TFs remained unaffected by knockdown of SOX4 in MDA-231 cells, with the exception of *ZEB2*, which increased in MDA-231 shSOX4 cells (< 2-fold, Supplementary Fig. 4D).

To determine to what extent SOX4 mediates the effects on gene expression that we observed in response to TRPM7 knockdown, we performed microarray analysis on MDA-231 shControl and shSOX4 cells, and compared the up- and downregulated genes between MDA-231 shTRPM7 and shSOX4 cells. Using as cut-off a 2-fold change, we found a highly significant overlap in up- and downregulated genes (135 upregulated genes, $p = 1.70e-97$ and 84 downregulated genes, $p = 5.01e-40$) (Fig. 3D & Supplementary Table 1). Additionally, rescue of SOX4 activity, by expression of a tamoxifen-inducible ER:SOX4 construct [51] in MDA-231 shTRPM7 cells, rescued mRNA and protein expression levels of E-cadherin, fibronectin and claudin-1 (Supplementary Fig. 5). Together, these data identify SOX4 as a key determinant of the TRPM7-induced gene expression signature. Moreover, our results indicate that activation of a TRPM7-SOX4 axis acts to preserve a mesenchymal-like state in breast cancer cells.

3.4. SOX4 expression is inversely correlated with cellular tension

We have shown previously that the TRPM7 kinase domain phosphorylates the myosin II heavy chain to inhibit myosin II-based cytoskeletal contraction [35,40]. Following the idea that cell mechanics control developmental gene expression programs [15,52–55], we hypothesized that TRPM7 may regulate SOX4 expression by modulating cellular tension.

Cellular tension is generated by contraction of the actomyosin cytoskeleton which is linked to the underlying substrate by cell-substrate adhesions. Typically, increased matrix stiffness activates an internal feedback loop that enforces sites of cell adhesion, promoting cell spreading and allowing active myosin to build up tension [10,12]. We applied traction force microscopy to quantitatively assess if and how TRPM7-mediated effects on myosin II activity modulate cellular tension. This technique is based on measurements of cell-induced substrate deformation by imaging displacements of fluorescent nanobeads embedded in the substrate [10,56]. MDA-231 shControl, shTRPM7 and shTRPM7#2 cells were cultured as single cells on collagen-coated substrates of different rigidities, covering physiologically relevant stiffness regimes (1–30 kPa) [17]. We observed that shControl cells generated more tension and elongated more efficiently when substrate stiffness increased (Fig. 4A–B). Supporting the notion that reduced TRPM7 expression increases cellular tension, MDA-231 shTRPM7 cells ($n > 30$ cells per condition) and shTRPM7#2 cells ($n > 15$ cells per condition) generated substantially more traction forces relative to shControl cells ($n > 30$ cells per condition) using substrates stiffer than 1 kPa (Fig. 4B; $p < 0{,}0001$, two-way ANOVA), without affecting cell surface area (Fig. 4C). Consistently, we observed that shTRPM7 cells formed larger focal adhesions on substrates stiffer than 1 kPa, when compared to shControl cells (Fig. 4D–E; $p < 0{,}0001$, two-way ANOVA, $n = 10$ cells per condition). Since focal adhesion reinforcement is driven by cellular tension, these results support the view that TRPM7 knockdown increases intracellular tension, independent of substrate stiffness.

To assess whether increased cytoskeletal tension is sufficient to reduce expression of SOX4, we stably transduced MDA-231 shControl cells with constitutive active RhoA (V14RhoA, Supplementary Fig. 6A), which activates actomyosin-based contraction by stimulation of the myosin light chain kinase [57]. Similar to TRPM7 knockdown cells, traction force measurements revealed that these cells generate more tension when compared to empty vector-transduced cells (Fig. 5A; $p < 0{,}0001$, two-way ANOVA, $n > 10$ cells per condition). Consistently, V14RhoA significantly reduced expression levels of SOX4 and fibronectin, and increased expression of claudin-1 (Fig. 5B–D). We also treated shControl cells with lysophosphatidic acid (LPA), a potent activator of RhoA [58], which similarly reduced the protein expression of SOX4 and increased expression of claudin-1 (Supplementary Fig. 6B–C). Since TRPM7 expression was not significantly affected by either V14RhoA or LPA, we can rule out the possibility that V14RhoA and LPA act by expression regulation of TRPM7. In contrast to TRPM7 and SOX4 knockdown (Figs. 1C & 3B), but similar to what we observed following Waix A treatment (Supplementary Fig. 1A), E-cadherin expression unexpectedly decreased in MDA-231 V14RhoA cells and after 8 h treatment with LPA (Fig. 5B & Supplementary Fig. 6B). At the same time, expression of the EMT-TF SNAI2 remained largely unaffected by increased cytoskeletal tension (Fig. 5B & Supplementary Fig. 6B). Together, these results demonstrate that increased cytoskeletal tension reduces SOX4 expression and downstream mesenchymal features, without bringing about a full MET.

We next determined to what extent reducing cytoskeletal tension can rescue SOX4 expression in MDA-231 shTRPM7 cells. To this end, we stimulated MDA-231 shTRPM7 cells with the myosin II ATPase inhibitor blebbistatin. Traction force measurements indicated that treatment of MDA-231 shTRPM7 cells with 10 μM blebbistatin reduced traction force generation to the level of shControl cells ($p < 0{,}0001$, two-way ANOVA, $n > 10$ cells per condition), whereas treatment with 25 μM blebbistatin almost completely blocked force generation on pliable substrates (Fig. 5E; $p < 0{,}0001$, two-way ANOVA, $n > 10$ cells per condition). This release of cellular tension was associated with a concordant increase in SOX4 and fibronectin expression levels, and reduced expression of claudin-1, whereas E-cadherin, SNAI2 and TRPM7 expression remained largely unaffected, indicating that TRPM7 controls SOX4 expression *via* the regulation of cytoskeletal tension

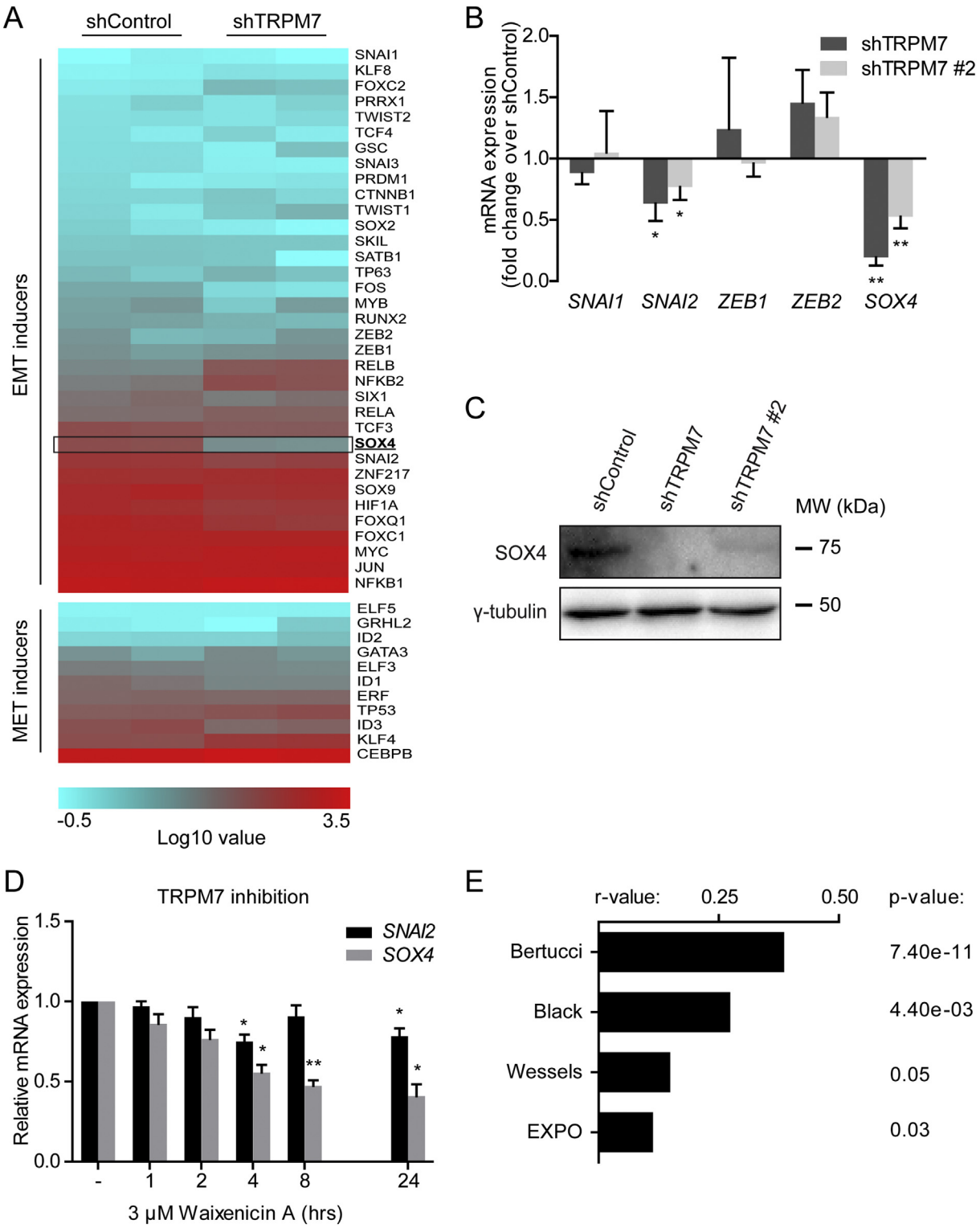

Fig. 2. TRPM7 knockdown reduces expression of the EMT transcription factor SOX4. (A) Microarray results depicted in a heatmap containing $\log_{10}$ transformed intensity values of known EMT and MET inducers in MDA-231 shControl and shTRPM7 cells. (B) Relative mRNA expression of well-established EMT-TFs, depicted as fold changes in expression over MDA-231 shControl. (C) Protein expression of SOX4 after stable knockdown of TRPM7, determined by Western blotting. Representative example of n = 3 experiments. (D) Effect of Waix A (3.3 μM) stimulation on *SOX4* and *SNAI2* mRNA expression in MDA-231 cells at different timepoints. Waix A activity is reduced in the presence of serum [48]. Therefore, stimulation was performed in serum-depleted medium. (B) and (D) mRNA expression levels were determined by q-PCR. Data are mean ± SEM of n = 3 experiments that were performed in duplicate. Statistical significance was determined by a one-sample *t*-test. * = $p < 0.05$, ** = $p < 0.01$. (E) Correlation coefficients between *TRPM7* and *SOX4* in four breast cancer patient datasets. Patient dataset analysis was performed using R2 microarray analysis tools (http://r2.amc.nl). Pearsons' correlations tests were performed to test for statistical significance of correlation.

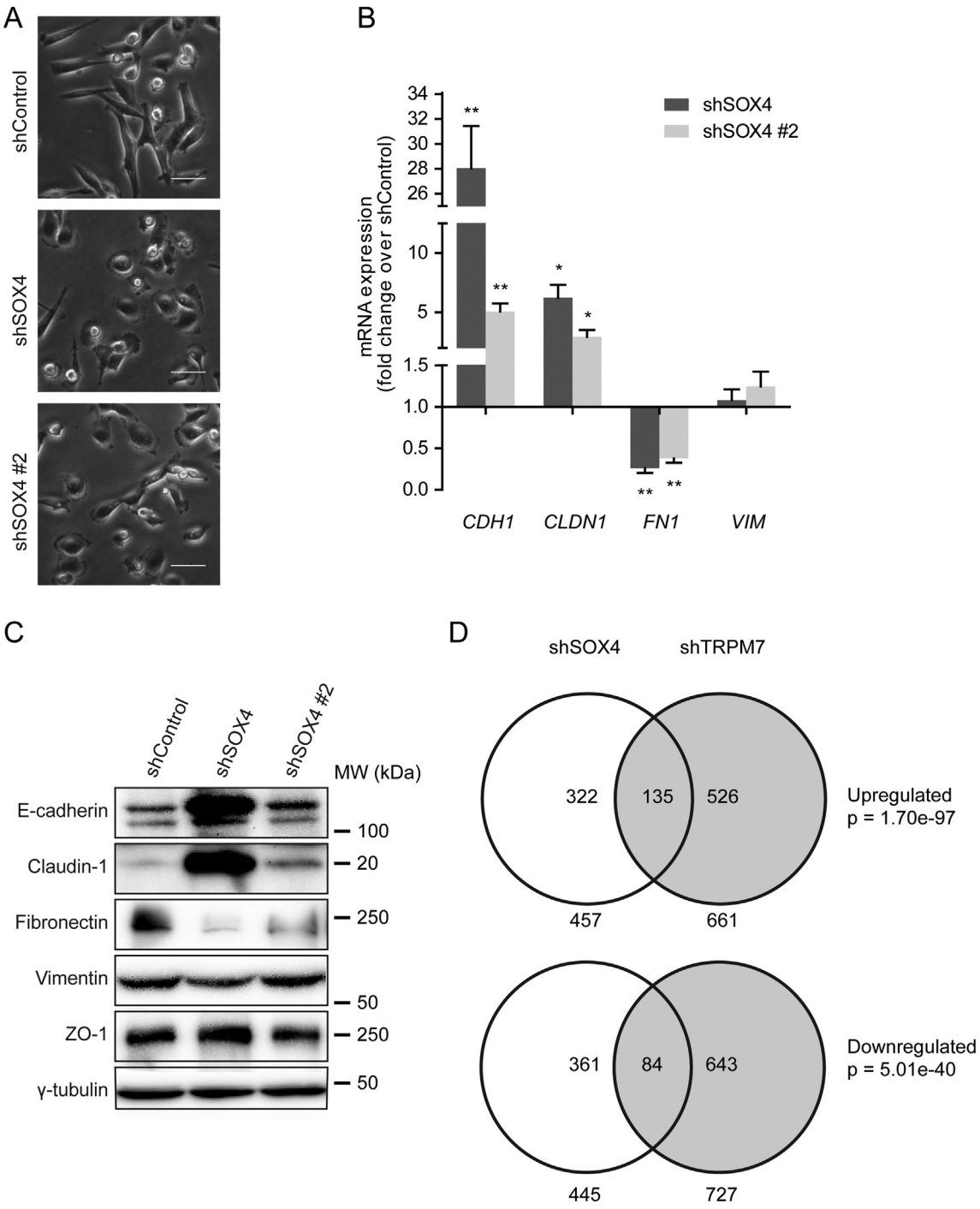

Fig. 3. SOX4 knockdown MDA-231 phenotypically mimic TRPM7 knockdown MDA-231. (A) Phase-contrast images showing morphology of MDA shControl, shSOX4 and shSOX4#2. Scale bar = 50 μM. (B) Relative mRNA expression of EMT markers, depicted as fold changes in expression over MDA-231 shControl as determined by q-PCR. Data are mean ± SEM of n = 3 experiments that were performed in duplicate. Statistical significance was determined by a one-sample *t*-test. * = $p < 0.05$, ** = $p < 0.01$. (C) Protein expression of EMT markers as determined by Western blotting. γ-Tubulin was used as loading control. Representative examples of n = 3 experiments. (D) Overlapping up- and downregulated genes in shSOX4#1 (total up: 457; total down: 445) and shT7#1 (total up: 661; total down: 727) microarray. A fold-change ≥ |2| was used as cut-off. p-Values were determined by means of a hypergeometric distribution test.

(Fig. 5F–H). Similar results were obtained when shTRPM7 cells were treated with the Rho-kinase inhibitor Y27632 (Supplementary Fig. 6D–E). Note that MDA-231 shControl cells were similarly responsive to Y27632 treatment (Supplementary Fig. 6D), in line with the notion that expression of these genes is primarily controlled by cytoskeletal tension rather than by TRPM7 expression levels. Importantly, inhibition of cytoskeletal tension induced a comparable mesenchymal phenotype in Hs 578T cells (Supplementary Fig. 6F).

Since increased substrate stiffness allows the build-up of tension by active myosin, we determined how cellular tension controls the expression of *SOX4*, *FN1* and *CLDN1* by seeding cells onto collagen-coated substrates with different rigidities. Consistent with the previous experiments, *SOX4* and *FN1* expression in MDA-231 shControl and shTRPM7 cells gradually decreased on stiffer matrices (Fig. 5I, p = 0,012 and p = 0,026 for *SOX4* and *FN1* respectively, two-way ANOVA, n = 5 independent experiments). Moreover, *CLDN1* expression

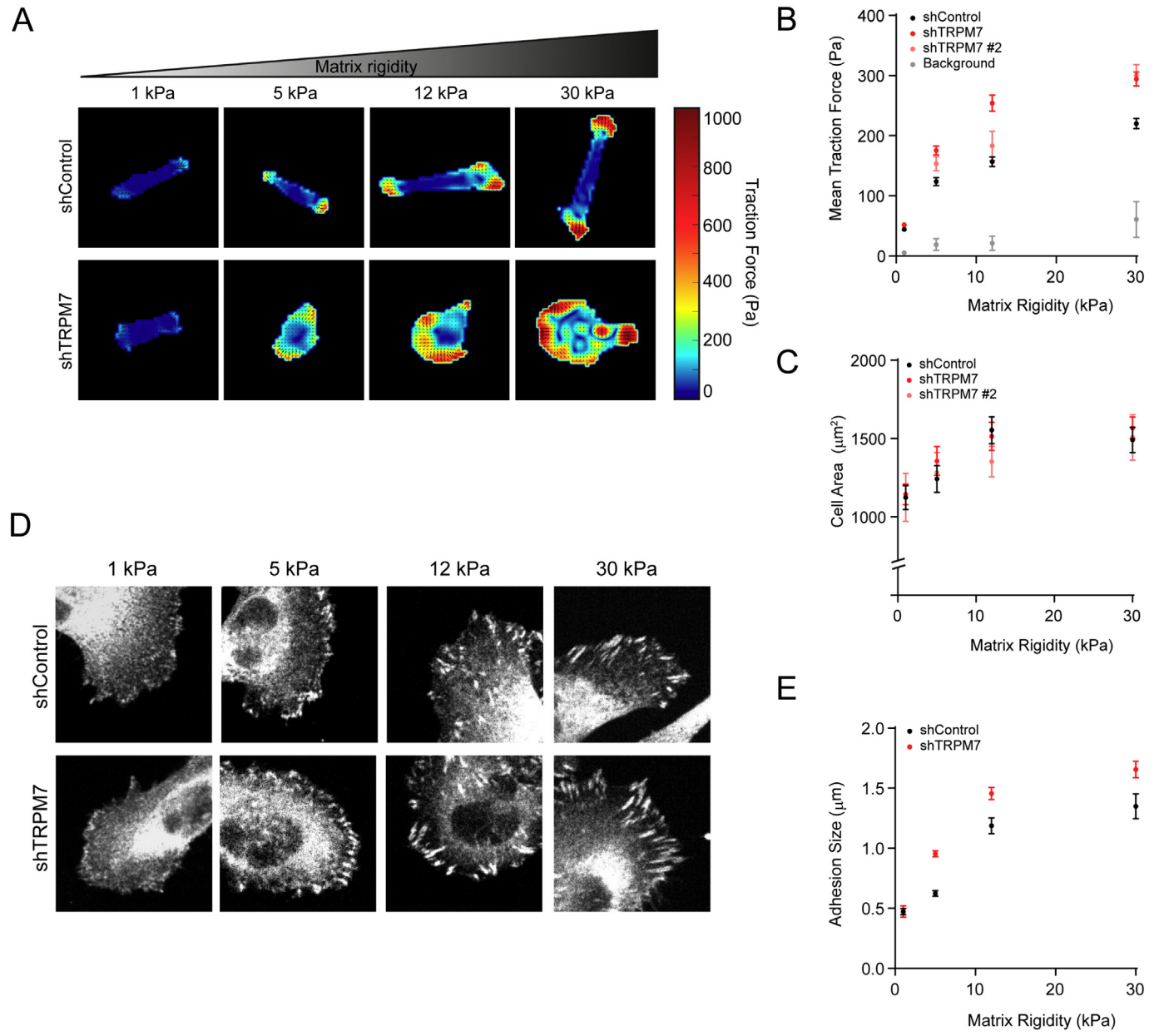

Fig. 4. TRPM7 knockdown increases cytoskeletal tension in MDA-231. (A) Color maps showing the traction forces applied to collagen-coated polyacrylamide gels of increasing rigidity by representative shControl and shTRPM7 MDA-231 cells. (B) Average traction forces exerted by single cells cultured on collagen coated polyacrylamide gels of increasing rigidity. In grey, background noise levels show the minimum detectable force for each rigidity value. (C) Average area of shControl and shTRPM7 MDA-231 cells seeded on collagen-coated polyacrylamide gels of increasing rigidity. (D) Representative examples of cell-substrate adhesions, revealed by anti-vinculin antibodies, in shControl and shTRPM7 MDA-231 cells cultured on polyacrylamide gels of increasing rigidity. (E) Quantification of vinculin adhesion length of single cells cultured on collagen-coated polyacrylamide gels of increasing rigidity.

strongly increased on stiff substrates (Fig. 5I, $p < 0{,}0001$, two-way ANOVA, $n = 5$ independent experiments). Taken together, our findings indicate that TRPM7 controls mesenchymal features of breast tumor cells by tensional regulation of SOX4.

4. Discussion

Cancer cells acquire progenitor-like features by re-activating developmental transcription programs such as EMT that promote metastasis and therapy resistance. There is mounting evidence that mechano-signaling affects such transcriptional programs. However, the molecular mechanisms involved remain incompletely understood [15,54,55]. We and others previously established that TRPM7, a cation channel with kinase activity and implicated in mechano-sensory processes, controls embryogenesis and drives tumor progression by regulating cytoskeletal dynamics [30–35,39–41,45]. Here, we show that TRPM7-induced cytoskeletal relaxation drives the mesenchymal features of breast tumor cells by promoting expression of the transcription factor SOX4, a recently identified regulator of EMT in breast cancer cells [43,44,59].

Consistent with promoting progenitor-like features in breast cancer cells, previous studies revealed that TRPM7 contributes to early embryonic development and organogenesis while it has been implicated in the maintenance of tissue homeostasis in the adult [31,32]. Clapham and colleagues reported an essential role for TRPM7 in neural crest development [32]. Neural crest cells arise when epithelial-like cells from the neuro-ectoderm undergo EMT to acquire migratory properties, allowing them to populate distinct parts of the embryo [60]. Tissue specific knockout experiments in mice revealed that TRPM7 expression

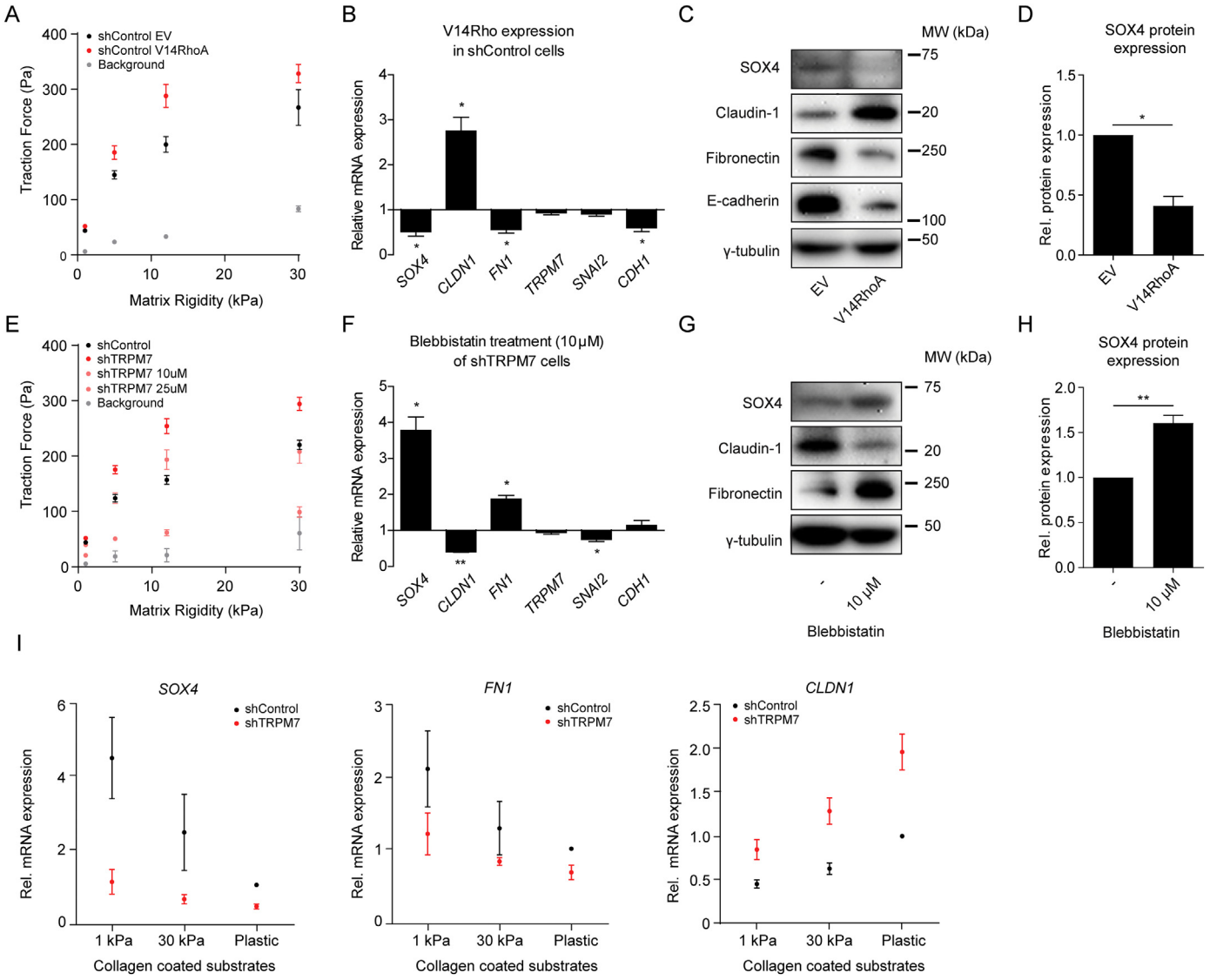

Fig. 5. SOX4 is inversely regulated by cytoskeletal tension. (A–D) Effect of stable overexpression of empty vector (EV) or V14RhoA in MDA-231 shControl cells on traction force generation (A), mRNA (B) and protein (C) expression of indicated genes. (D) Quantification of SOX4 protein expression upon overexpression of V14RhoA. To enhance SOX4 protein expression, MDA-231 EV and V14RhoA cells were incubated in medium containing 0.1% FCS for 16 h before protein lysate was harvested. (E–H) Effect of myosin II inhibition in MDA-231 shTRPM7#1 on traction force generation (E), mRNA (F) and protein (G) expression of indicated genes. (H) Quantification of SOX4 protein expression after myosin II inhibition. MDA-231 shTRPM7 cells were stimulated with DMSO vehicle or indicated concentrations blebbistatin for 2 h to quantify effects on traction force generation. To measure effects of blebbistatin on mRNA and protein expression, cells were treated with 10 μM blebbistatin for 2 consecutive days or 16 h, respectively. (I) Effect of matrix rigidity on *SOX4*, *FN1 and CLDN1* mRNA expression in MDA-231 shControl and shTRPM7 cells. Cells were seeded onto collagen-coated substrates with indicated rigidities and cultured for 72 h. (A & E) Traction force generation was determined by traction force microscopy on $n > 10$ cells per condition. Significance was tested using a two-way ANOVA. (B, F & I) mRNA expression levels were determined by q-PCR. Data are mean ± SEM of $n = 3$ (B & F) or $n = 5$ (I) experiments that were performed in duplicate. Statistical significance was determined by a one-sample *t*-test (B & F) and a two-way ANOVA (G). * = $p < 0.05$, ** = $p < 0.01$. (C & G) Protein levels of EMT markers were determined by Western blotting. γ-Tubulin was used as loading control. Representative examples of $n = 3$ experiments are shown. (D & H) SOX4 protein levels were normalized to the γ-tubulin loading control. Data are mean ± SEM of $n = 3$. Statistical significance was determined by a one-sample *t*-test. * = $p < 0.05$, ** = $p < 0.01$.

is required for maintaining neural crest cells in a progenitor-like, migratory state during embryogenesis [32]. In addition, we showed that TRPM7 maintains progenitor-like features of neuroblastoma cells, tumor cells derived from poorly differentiated neural crest cells, by promoting the expression of the EMT-TF SNAI2 [39]. Furthermore, our results are in accordance with findings showing that TRPM7 is able to regulate protein expression of the EMT marker vimentin in MDA-MB-468 breast cancer cells [47]. Altogether, these findings point to a role for TRPM7 as a regulator of EMT-like transcriptional programs during embryogenesis and tumor progression.

Based on biochemical and cell biological evidence, we previously put forward that TRPM7 directly inhibits myosin II function by phosphorylating the myosin II heavy chain, resulting in disassembly of bipolar myosin II filaments [35,40]. Here, we applied traction force microscopy confirming that knockdown of TRPM7 increases cellular tension. Interestingly, we find that the expression of SOX4, and the majority of its downstream mesenchymal effectors, is inversely correlated with cellular tension, while expression of other EMT-TF factors remains unaffected. Moreover, we were able to (partially) restore the phenotypical consequences of TRPM7 knockdown by inhibiting cytoskeletal contraction, indicating that TRPM7 regulates gene expression by modulating cytoskeletal contraction. Surprisingly however, expression of the epithelial marker E-cadherin (*CDH1*) was downregulated upon temporary inhibition of TRPM7 or induction of cellular tension, while

E-cadherin expression was upregulated both in TRPM7 shRNA and SOX4 shRNA cells. We speculate that a more sustained decrease in TRPM7 activity, as observed in response to shRNA-mediated knockdown, is required to induce *CDH1* expression. In contrast to previous studies, modulation of SOX4 expression did not affect N-cadherin expression in our breast cancer cell models. However, cell plasticity is not a binary process (on/off) but reflects context dependent activation of different gene expression programs that control cell survival, proliferation and cell motility [61]). Consequently, different cell types may respond differently to the same input.

Since TRPM7 localizes to cell-substrate adhesions and controls cellular tension, our data support a model in which TRPM7 is part of a unique mechanical signaling hub that controls cell plasticity at the level of gene expression, and contributes to tissue development and maintenance. How cytoskeletal relaxation promotes SOX4 expression remains to be established. Possibly, cytoskeletal relaxation maintains and/or enhances nuclear localization of a yet to be determined transcriptional regulator. A similar mechanism has been described for the transcriptional regulators YAP and TAZ, which translocate to the nucleus in response to increased cytoskeletal tension [14]. Alternatively, cytoskeletal tension may be transmitted directly to the nucleus, affecting tension on the nuclear membrane and consequently chromatin organization, which in turn may affect transcription [15,62].

It is well known that the mechanical properties of the tumor microenvironment affect the metastatic capabilities of tumor cells [17,54,55,63]. High tumor stiffness is generally considered to promote tumor development and progression [22,63,64]. Although our observations need confirmation using experimental models that represent tumor progression in the patient, they challenge this model by showing that limiting cell contractility can also lead to activation of transcription programs driving metastasis and therapy resistance. In support of our findings, a number of papers report that low cellular tension and softness is correlated with metastatic features and a mesenchymal phenotype at the cellular level, as well as disease progression in cancer patients [65–72]. For instance, EMT induces cellular softness in both endometrial and breast cancer cells [68,73]. Additionally, although high mammographic density increases the risk of breast cancer development [74], very low mammographic density (< 10%) correlates with poor patient survival, prognosis and histological tumor grade [75–77]. It was furthermore shown in late-stage breast tumors that, although the periphery of primary tumors is stiffer than healthy breast tissue, the hypoxic core is in fact softer than healthy counterparts [66]. Consistently, migration and metastatic spreading were positively correlated with the low stiffness of these hypoxic core-associated cells [66]. Combined, these results suggest that low mammographic density and decreased cellular tension at later stages of tumor progression in fact promote metastasis formation and poor outcome. Hence, it appears that, dependent on cellular context and disease stage, both high and low cellular tension can contribute to tumor progression.

In the past few years, the importance of epithelial to mesenchymal plasticity, particularly with respect to invasion and metastasis, has been subject to debate [61]. We observe that loss of cytoskeletal tension contributes to at least some mesenchymal features in our breast cancer model, while we have shown previously that high *TRPM7* expression is correlated with metastatic behavior of breast cancer cells [35]. Altogether our data imply that breast cancer-associated plasticity is affected by both tissue rigidity and the tensional state of tumor cells, which appears to involve the tensional regulation of SOX4 expression by TRPM7. In this cellular context, limiting the contractile response to tissue stiffness may therefore promote rather than inhibit metastasis formation.

Supplementary data to this article can be found online at https://doi.org/10.1016/j.bbadis.2018.04.017.

Transparency document

The http://dx.doi.org/10.1016/j.bbadis.2018.04.017 associated with this article can be found, in online version.

Acknowledgements

We thank Prof. P.J. Coffer (UMC-Utrecht, Utrecht, The Netherlands) for sharing the pBABE-blast ER and pBABE-blast ER:SOX4 constructs. This work is supported by a KWF grant to KJ & FvL (NKI 2010-4626), a Radboudumc PhD scholarship to KV and EMBO and FEBS short-term grants to JM. CP-G was supported by fundació 'La Caixa'. XT is funded by the Spanish Ministry of Economy, Industry and Competitiveness through the Centro de Excelencia Severo Ochoa Award to the Institute of Bioengineering of Catalonia and through grant BFU2015-65074-P, the Generalitat de Catalunya (Cerca Program and 2014-SGR-927), the European Research Council (CoG-616480), and the European Commission (project 731957).

Conflict of interest

The authors declare no conflict of interest.

References

[1] B. Trappmann, J.E. Gautrot, J.T. Connelly, D.G. Strange, Y. Li, M.L. Oyen, M.A. Cohen Stuart, H. Boehm, B. Li, V. Vogel, J.P. Spatz, F.M. Watt, W.T. Huck, Extracellular-matrix tethering regulates stem-cell fate, Nat. Mater. 11 (2012) 642–649.
[2] A.J. Engler, S. Sen, H.L. Sweeney, D.E. Discher, Matrix elasticity directs stem cell lineage specification, Cell 126 (2006) 677–689.
[3] E. Bellas, C.S. Chen, Forms, forces, and stem cell fate, Curr. Opin. Cell Biol. 31 (2014) 92–97.
[4] T. Mammoto, A. Mammoto, D.E. Ingber, Mechanobiology and developmental control, Annu. Rev. Cell Dev. Biol. 29 (2013) 27–61.
[5] R. McBeath, D.M. Pirone, C.M. Nelson, K. Bhadriraju, C.S. Chen, Cell shape, cytoskeletal tension, and RhoA regulate stem cell lineage commitment, Dev. Cell 6 (2004) 483–495.
[6] D.E. Jaalouk, J. Lammerding, Mechanotransduction gone awry, Nat. Rev. Mol. Cell Biol. 10 (2009) 63–73.
[7] C.S. Chen, M. Mrksich, S. Huang, G.M. Whitesides, D.E. Ingber, Geometric control of cell life and death, Science 276 (1997) 1425–1428.
[8] C.C. DuFort, M.J. Paszek, V.M. Weaver, Balancing forces: architectural control of mechanotransduction, Nat. Rev. Mol. Cell Biol. 12 (2011) 308–319.
[9] D.E. Ingber, Mechanobiology and diseases of mechanotransduction, Ann. Med. 35 (2003) 564–577.
[10] A. Elosegui-Artola, E. Bazellieres, M.D. Allen, I. Andreu, R. Oria, R. Sunyer, J.J. Gomm, J.F. Marshall, J.L. Jones, X. Trepat, P. Roca-Cusachs, Rigidity sensing and adaptation through regulation of integrin types, Nat. Mater. 13 (2014) 631–637.
[11] J. Eyckmans, T. Boudou, X. Yu, C.S. Chen, A hitchhiker's guide to mechanobiology, Dev. Cell 21 (2011) 35–47.
[12] D. Riveline, E. Zamir, N.Q. Balaban, U.S. Schwarz, T. Ishizaki, S. Narumiya, Z. Kam, B. Geiger, A.D. Bershadsky, Focal contacts as mechanosensors: externally applied local mechanical force induces growth of focal contacts by an mDia1-dependent and ROCK-independent mechanism, J. Cell Biol. 153 (2001) 1175–1186.
[13] E. Bazellieres, V. Conte, A. Elosegui-Artola, X. Serra-Picamal, M. Bintanel-Morcillo, P. Roca-Cusachs, J.J. Munoz, M. Sales-Pardo, R. Guimera, X. Trepat, Control of cell-cell forces and collective cell dynamics by the intercellular adhesome, Nat. Cell Biol. 17 (2015) 409–420.
[14] S. Dupont, L. Morsut, M. Aragona, E. Enzo, S. Giulitti, M. Cordenonsi, F. Zanconato, J. Le Digabel, M. Forcato, S. Bicciato, N. Elvassore, S. Piccolo, Role of YAP/TAZ in mechanotransduction, Nature 474 (2011) 179–183.
[15] A. Mammoto, T. Mammoto, D.E. Ingber, Mechanosensitive mechanisms in transcriptional regulation, J. Cell Sci. 125 (2012) 3061–3073.
[16] F. Miralles, G. Posern, A.I. Zaromytidou, R. Treisman, Actin dynamics control SRF activity by regulation of its coactivator MAL, Cell 113 (2003) 329–342.
[17] M.J. Paszek, N. Zahir, K.R. Johnson, J.N. Lakins, G.I. Rozenberg, A. Gefen, C.A. Reinhart-King, S.S. Margulies, M. Dembo, D. Boettiger, D.A. Hammer, V.M. Weaver, Tensional homeostasis and the malignant phenotype, Cancer Cell 8 (2005) 241–254.
[18] S. Huang, D.E. Ingber, Cell tension, matrix mechanics, and cancer development, Cancer Cell 8 (2005) 175–176.
[19] M.W. Pickup, J.K. Mouw, V.M. Weaver, The extracellular matrix modulates the hallmarks of cancer, EMBO Rep. 15 (2014) 1243–1253.
[20] S. Medjkane, C. Perez-Sanchez, C. Gaggioli, E. Sahai, R. Treisman, Myocardin-related transcription factors and SRF are required for cytoskeletal dynamics and experimental metastasis, Nat. Cell Biol. 11 (2009) 257–268.
[21] M. Cordenonsi, F. Zanconato, L. Azzolin, M. Forcato, A. Rosato, C. Frasson, M. Inui, M. Montagner, A.R. Parenti, A. Poletti, M.G. Daidone, S. Dupont, G. Basso, S. Bicciato, S. Piccolo, The Hippo transducer TAZ confers cancer stem cell-related

traits on breast cancer cells, Cell 147 (2011) 759–772.
[22] S.C. Wei, L. Fattet, J.H. Tsai, Y. Guo, V.H. Pai, H.E. Majeski, A.C. Chen, R.L. Sah, S.S. Taylor, A.J. Engler, J. Yang, Matrix stiffness drives epithelial-mesenchymal transition and tumour metastasis through a TWIST1-G3BP2 mechanotransduction pathway, Nat. Cell Biol. 17 (2015) 678–688.
[23] D.M. Gonzalez, D. Medici, Signaling mechanisms of the epithelial-mesenchymal transition, Sci. Signal. 7 (2014) re8.
[24] L. Seguin, J.S. Desgrosellier, S.M. Weis, D.A. Cheresh, Integrins and cancer: regulators of cancer stemness, metastasis, and drug resistance, Trends Cell Biol. 25 (2015) 234–240.
[25] J.P. Thiery, H. Acloque, R.Y. Huang, M.A. Nieto, Epithelial-mesenchymal transitions in development and disease, Cell 139 (2009) 871–890.
[26] K.S. Vrenken, K. Jalink, F.N. van Leeuwen, J. Middelbeek, Beyond ion-conduction: channel-dependent and -independent roles of TRP channels during development and tissue homeostasis, Biochim. Biophys. Acta 1863 ((2016) 1436–1446.
[27] A.J. Kuipers, J. Middelbeek, F.N. van Leeuwen, Mechanoregulation of cytoskeletal dynamics by TRP channels, Eur. J. Cell Biol. 91 (2012) 834–846.
[28] P. Delmas, B. Coste, Mechano-gated ion channels in sensory systems, Cell 155 (2013) 278–284.
[29] K. Clark, J. Middelbeek, F.N. van Leeuwen, Interplay between TRP channels and the cytoskeleton in health and disease, Eur. J. Cell Biol. 87 (2008) 631–640.
[30] D. Visser, J. Middelbeek, F.N. van Leeuwen, K. Jalink, Function and regulation of the channel-kinase TRPM7 in health and disease, Eur. J. Cell Biol. 93 (2014) 455–465.
[31] J. Jin, B.N. Desai, B. Navarro, A. Donovan, N.C. Andrews, D.E. Clapham, Deletion of Trpm7 disrupts embryonic development and thymopoiesis without altering Mg^{2+} homeostasis, Science 322 (2008) 756–760.
[32] J. Jin, L.J. Wu, J. Jun, X. Cheng, H. Xu, N.C. Andrews, D.E. Clapham, The channel kinase, TRPM7, is required for early embryonic development, Proc. Natl. Acad. Sci. U. S. A. 109 (2012) E225–233.
[33] W. Liu, L.T. Su, D.K. Khadka, C. Mezzacappa, Y. Komiya, A. Sato, R. Habas, L.W. Runnels, TRPM7 regulates gastrulation during vertebrate embryogenesis, Dev. Biol. 350 (2011) 348–357.
[34] M.R. Elizondo, B.L. Arduini, J. Paulsen, E.L. MacDonald, J.L. Sabel, P.D. Henion, R.A. Cornell, D.M. Parichy, Defective skeletogenesis with kidney stone formation in dwarf zebrafish mutant for trpm7, Curr. Biol. CB 15 (2005) 667–671.
[35] J. Middelbeek, A.J. Kuipers, L. Henneman, D. Visser, I. Eidhof, R. van Horssen, B. Wieringa, S.V. Canisius, W. Zwart, L.F. Wessels, F.C. Sweep, P. Bult, P.N. Span, F.N. van Leeuwen, K. Jalink, TRPM7 is required for breast tumor cell metastasis, Cancer Res. 72 (2012) 4250–4261.
[36] P. Rybarczyk, M. Gautier, F. Hague, I. Dhennin-Duthille, D. Chatelain, J. Kerr-Conte, F. Pattou, J.M. Regimbeau, H. Sevestre, H. Ouadid-Ahidouch, Transient receptor potential melastatin-related 7 channel is overexpressed in human pancreatic ductal adenocarcinomas and regulates human pancreatic cancer cell migration, Int. J. Cancer. Journal international du cancer 131 (2012) E851–861.
[37] Y. Sun, S. Selvaraj, A. Varma, S. Derry, A.E. Sahmoun, B.B. Singh, Increase in serum Ca^{2+}/Mg^{2+} ratio promotes proliferation of prostate cancer cells by activating TRPM7 channels, J. Biol. Chem. 288 (2013) 255–263.
[38] J.P. Chen, J. Wang, Y. Luan, C.X. Wang, W.H. Li, J.B. Zhang, D. Sha, R. Shen, Y.G. Cui, Z. Zhang, L.M. Zhang, W.B. Wang, TRPM7 promotes the metastatic process in human nasopharyngeal carcinoma, Cancer Lett. 356 (2015) 483–490.
[39] J. Middelbeek, D. Visser, L. Henneman, A. Kamermans, A.J. Kuipers, P.M. Hoogerbrugge, K. Jalink, F.N. van Leeuwen, TRPM7 maintains progenitor-like features of neuroblastoma cells: implications for metastasis formation, Oncotarget 6 (2015) 8760–8776.
[40] K. Clark, M. Langeslag, B. van Leeuwen, L. Ran, A.G. Ryazanov, C.G. Figdor, W.H. Moolenaar, K. Jalink, F.N. van Leeuwen, TRPM7, a novel regulator of actomyosin contractility and cell adhesion, EMBO J. 25 (2006) 290–301.
[41] L.T. Su, M.A. Agapito, M. Li, W.T. Simonson, A. Huttenlocher, R. Habas, L. Yue, L.W. Runnels, TRPM7 regulates cell adhesion by controlling the calcium-dependent protease calpain, J. Biol. Chem. 281 (2006) 11260–11270.
[42] D. Visser, M. Langeslag, K.M. Kedziora, J. Klarenbeek, A. Kamermans, F.D. Horgen, A. Fleig, F.N. van Leeuwen, K. Jalink, TRPM7 triggers Ca^{2+} sparks and invadosome formation in neuroblastoma cells, Cell Calcium 54 (2013) 404–415.
[43] N. Tiwari, V.K. Tiwari, L. Waldmeier, P.J. Balwierz, P. Arnold, M. Pachkov, N. Meyer-Schaller, D. Schubeler, E. van Nimwegen, G. Christofori, Sox4 is a master regulator of epithelial-mesenchymal transition by controlling Ezh2 expression and epigenetic reprogramming, Cancer Cell 23 (2013) 768–783.
[44] S.J. Vervoort, R. van Boxtel, P.J. Coffer, The role of SRY-related HMG box transcription factor 4 (SOX4) in tumorigenesis and metastasis: friend or foe? Oncogene 32 (2013) 3397–3409.
[45] J. Du, J. Xie, Z. Zhang, H. Tsujikawa, D. Fusco, D. Silverman, B. Liang, L. Yue, TRPM7-mediated Ca^{2+} signals confer fibrogenesis in human atrial fibrillation, Circ. Res. 106 (2010) 992–1003.
[46] R. Cao, Z. Meng, T. Liu, G. Wang, G. Qian, T. Cao, X. Guan, H. Dan, Y. Xiao, X. Wang, Decreased TRPM7 inhibits activities and induces apoptosis of bladder cancer cells via ERK1/2 pathway, Oncotarget 7 (2016) 72941–72960.
[47] F.M. Davis, I. Azimi, R.A. Faville, A.A. Peters, K. Jalink, J.W. Putney Jr., G.J. Goodhill, E.W. Thompson, S.J. Roberts-Thomson, G.R. Monteith, Induction of epithelial-mesenchymal transition (EMT) in breast cancer cells is calcium signal dependent, Oncogene 33 (2014) 2307–2316.
[48] S. Zierler, G. Yao, Z. Zhang, W.C. Kuo, P. Porzgen, R. Penner, F.D. Horgen, A. Fleig, Waixenicin A inhibits cell proliferation through magnesium-dependent block of transient receptor potential melastatin 7 (TRPM7) channels, J. Biol. Chem. 286 (2011) 39328–39335.
[49] S. Lamouille, J. Xu, R. Derynck, Molecular mechanisms of epithelial-mesenchymal transition, Nat. Rev. Mol. Cell Biol. 15 (2014) 178–196.
[50] A. Moustakas, P. Heldin, TGFbeta and matrix-regulated epithelial to mesenchymal transition, Biochim. Biophys. Acta 1840 (2014) 2621–2634.
[51] S.J. Vervoort, A.R. Lourenco, R. van Boxtel, P.J. Coffer, SOX4 mediates TGF-beta-induced expression of mesenchymal markers during mammary cell epithelial to mesenchymal transition, PLoS One 8 (2013) e53238.
[52] G. Halder, S. Dupont, S. Piccolo, Transduction of mechanical and cytoskeletal cues by YAP and TAZ, Nat. Rev. Mol. Cell Biol. 13 (2012) 591–600.
[53] G. Posern, R. Treisman, Actin' together: serum response factor, its cofactors and the link to signal transduction, Trends Cell Biol. 16 (2006) 588–596.
[54] L. Przybyla, J.M. Muncie, V.M. Weaver, Mechanical control of epithelial-to-mesenchymal transitions in development and cancer, Annu. Rev. Cell Dev. Biol. 32 (2016) 527–554.
[55] S.C. Wei, J. Yang, Forcing through tumor metastasis: the interplay between tissue rigidity and epithelial-mesenchymal transition, Trends Cell Biol. 26 (2016) 111–120.
[56] J.P. Butler, I.M. Tolic-Norrelykke, B. Fabry, J.J. Fredberg, Traction fields, moments, and strain energy that cells exert on their surroundings, Am. J. Phys. Cell Phys. 282 (2002) C595–605.
[57] K. Clark, M. Langeslag, C.G. Figdor, F.N. van Leeuwen, Myosin II and mechanotransduction: a balancing act, Trends Cell Biol. 17 (2007) 178–186.
[58] W.H. Moolenaar, L.A. van Meeteren, B.N. Giepmans, The ins and outs of lysophosphatidic acid signaling, bioessays: news and reviews in molecular, Cell. Dev. Biol. 26 (2004) 870–881.
[59] J. Zhang, Q. Liang, Y. Lei, M. Yao, L. Li, X. Gao, J. Feng, Y. Zhang, H. Gao, D.X. Liu, J. Lu, B. Huang, SOX4 induces epithelial-mesenchymal transition and contributes to breast cancer progression, Cancer Res. 72 (2012) 4597–4608.
[60] M.S. Prasad, T. Sauka-Spengler, C. LaBonne, Induction of the neural crest state: control of stem cell attributes by gene regulatory, post-transcriptional and epigenetic interactions, Dev. Biol. 366 (2012) 10–21.
[61] X. Ye, T. Brabletz, Y. Kang, G.D. Longmore, M.A. Nieto, B.Z. Stanger, J. Yang, R.A. Weinberg, Upholding a role for EMT in breast cancer metastasis, Nature 547 (2017) E1–E3.
[62] H.Q. Le, S. Ghatak, C.Y. Yeung, F. Tellkamp, C. Gunschmann, C. Dieterich, A. Yeroslaviz, B. Habermann, A. Pombo, C.M. Niessen, S.A. Wickstrom, Mechanical regulation of transcription controls Polycomb-mediated gene silencing during lineage commitment, Nat. Cell Biol. 18 (2016) 864–875.
[63] D.T. Butcher, T. Alliston, V.M. Weaver, A tense situation: forcing tumour progression, Nat. Rev. Cancer 9 (2009) 108–122.
[64] P.P. Provenzano, D.R. Inman, K.W. Eliceiri, P.J. Keely, Matrix density-induced mechanoregulation of breast cell phenotype, signaling and gene expression through a FAK-ERK linkage, Oncogene 28 (2009) 4326–4343.
[65] Y. Tan, A. Tajik, J. Chen, Q. Jia, F. Chowdhury, L. Wang, J. Chen, S. Zhang, Y. Hong, H. Yi, D.C. Wu, Y. Zhang, F. Wei, Y.C. Poh, J. Seong, R. Singh, L.J. Lin, S. Doganay, Y. Li, H. Jia, T. Ha, Y. Wang, B. Huang, N. Wang, Matrix softness regulates plasticity of tumour-repopulating cells via H3K9 demethylation and Sox2 expression, Nat. Commun. 5 (2014) 4619.
[66] M. Plodinec, M. Loparic, C.A. Monnier, E.C. Obermann, R. Zanetti-Dallenbach, P. Oertle, J.T. Hyotyla, U. Aebi, M. Bentires-Alj, R.Y. Lim, C.A. Schoenenberger, The nanomechanical signature of breast cancer, Nat. Nanotechnol. 7 (2012) 757–765.
[67] D.J. McGrail, Q.M. Kieu, M.R. Dawson, The malignancy of metastatic ovarian cancer cells is increased on soft matrices through a mechanosensitive Rho-ROCK pathway, J. Cell Sci. 127 (2014) 2621–2626.
[68] Y.T. Hsu, P. Osmulski, Y. Wang, Y.W. Huang, L. Liu, J. Ruan, V.X. Jin, N.B. Kirma, M.E. Gaczynska, T.H. Huang, EpCAM-regulated transcription exerts influences on nanomechanical properties of endometrial cancer cells that promote epithelial-to-mesenchymal transition, Cancer Res. 76 (2016) 6171–6182.
[69] E.A. Corbin, F. Kong, C.T. Lim, W.P. King, R. Bashir, Biophysical properties of human breast cancer cells measured using silicon MEMS resonators and atomic force microscopy, Lab Chip 15 (2015) 839–847.
[70] Q.S. Li, G.Y. Lee, C.N. Ong, C.T. Lim, AFM indentation study of breast cancer cells, Biochem. Biophys. Res. Commun. 374 (2008) 609–613.
[71] S.E. Cross, Y.S. Jin, J. Rao, J.K. Gimzewski, Nanomechanical analysis of cells from cancer patients, Nat. Nanotechnol. 2 (2007) 780–783.
[72] V. Swaminathan, K. Mythreye, E.T. O'Brien, A. Berchuck, G.C. Blobe, R. Superfine, Mechanical stiffness grades metastatic potential in patient tumor cells and in cancer cell lines, Cancer Res. 71 (2011) 5075–5080.
[73] D.J. McGrail, R. Mezencev, Q.M. Kieu, J.F. McDonald, M.R. Dawson, SNAIL-induced epithelial-to-mesenchymal transition produces concerted biophysical changes from altered cytoskeletal gene expression, FASEB J. 29 (2015) 1280–1289.
[74] U. Veronesi, P. Boyle, A. Goldhirsch, R. Orecchia, G. Viale, Breast cancer, Lancet 365 (2005) 1727–1741.
[75] A. Masarwah, P. Auvinen, M. Sudah, S. Rautiainen, A. Sutela, O. Pelkonen, S. Oikari, V.M. Kosma, R. Vanninen, Very low mammographic breast density predicts poorer outcome in patients with invasive breast cancer, Eur. Radiol. 25 (2015) 1875–1882.
[76] A. Masarwah, M. Tammi, M. Sudah, A. Sutela, S. Oikari, V.M. Kosma, R. Tammi, R. Vanninen, P. Auvinen, The reciprocal association between mammographic breast density, hyaluronan synthesis and patient outcome, Breast Cancer Res. Treat. 153 (2015) 625–634.
[77] A.H. Olsen, K. Bihrmann, M.B. Jensen, I. Vejborg, E. Lynge, Breast density and outcome of mammography screening: a cohort study, Br. J. Cancer 100 (2009) 1205–1208.
[78] X. Serra-Picamal, V. Conte, R. Vincent, E. Anon, D.T. Tambe, E. Bazellieres, J.P. Butler, J.J. Fredberg, X. Trepat, Mechanical waves during tissue expansion, Nat. Phys. 8 (2012) 628–634.
[79] P. Roca-Cusachs, J. Alcaraz, R. Sunyer, J. Samitier, R. Farre, D. Navajas, Micropatterning of single endothelial cell shape reveals a tight coupling between nuclear volume in G1 and proliferation, Biophys. J. 94 (2008) 4984–4995.